

Improving tidal turbine array performance through the optimisation of layout and yaw angles

Can Zhang, Stephan C. Kramer, Athanasios Angeloudis, Jisheng Zhang, Xiangfeng Lin, and Matthew D. Piggott

Abstract—Tidal stream currents change in magnitude and direction during flood and ebb tides. Setting the most appropriate yaw angles for a tidal turbine is not only important to account for the performance of a single turbine, but can also be significant for the interactions between the turbines within an array. In this paper, a partial differentiation equation (PDE) constrained optimisation approach is established based on the Thetis coastal ocean modelling framework. The PDE constraint takes the form here of the two-dimensional, depth-averaged shallow water equations which are used to simulate tidal elevations and currents in the presence of tidal stream turbine arrays. The Sequential Least Squares Programming (SLSQP) algorithm is applied with a gradient obtained via the adjoint method in order to perform array design optimisation. An idealised rectangular channel test case is studied to demonstrate this optimisation framework. Located in the centre of the computational domain, arrays comprised of 12 turbines are tested in aligned and staggered layouts. The setups are initially optimised based on their yaw angles alone. In turn, turbine coordinates and yaw angles are also optimized simultaneously. Results indicate that for an aligned turbine array case under steady state conditions, the energy output

can be increased by approximately 80% when considering yaw angle optimisation alone. For the staggered turbine array, the increase is approximately 30%. The yaw optimised staggered array is able to outperform the yaw optimised aligned array by approximately 8%. If both layout and the yaw angles of the turbines are considered within the optimisation then the increase is more significant compared with optimising yaw angle alone.

Index Terms—Tidal stream energy, Shallow water equation, Yaw angle, Layout, Optimisation

I. INTRODUCTION

TIDAL stream energy represents a renewable energy source that can contribute to mitigating the global energy crisis, with researchers and developers actively working on methods to harness it and quantify it effectively [1]. In particular, horizontal axis turbines are the most common devices considered for tidal stream energy extraction. The amount of tidal stream energy generated by a turbine is directly proportional to the product of the turbine swept area and the cube of the tidal velocity [2]. Thus, the obvious way to improve the extraction of tidal stream energy from a channel is to increase the total swept area by increasing the number of turbines that form an array. The optimal positioning of turbines within an array (micro-siting) however, taking into account blockage effects and the interaction between the wake of a turbine with turbines downstream, is a complex problem. As well as its layout, another aspect that impacts the combined performance of a turbine array is the orientation of turbines with respect to the tidal stream, known as the yaw angle. The yaw angle of each turbine individually not only affects the amount of energy that can be extracted by the turbine itself, but may affect the available energy for downstream turbines through wake steering effects.

Tidal turbine array layout optimisation has been studied in a number of recent publications. Some newly developed methods have demonstrated that the array efficiency can be increased significantly through careful positioning of turbines within an array [3], [4]. For example, González-Gorbeña et al. [5] applied a surrogate-based optimisation for tidal turbine arrays in the Faro-Olhao to specify the optimum separation constraints within the array layout. For a scenario where 30 turbines were deployed, they found an optimal configuration of three rows of ten turbines. Wu et al. [6] used a discrete particle swarm algorithm to optimise

This paper was submitted on 27 December, 2021; published 19 December 2022. This is an open access article distributed under the terms of the Creative Commons Attribution 4.0 licence (CC BY <http://creativecommons.org/licenses/by/4.0/>). Unrestricted use (including commercial), distribution and reproduction is permitted provided that credit is given to the original author(s) of the work, including a URI or hyperlink to the work, this public license and a copyright notice. This article has been subject to single-blind peer review by a minimum of two reviewers.

The authors are grateful for sponsorship from the China Scholarship Council (No. 201906710084), the Fundamental Research Funds for the Central Universities (B210203022), the National Natural Science Foundation of China (51879098), and the Marine Renewable Energy Research Project of State Oceanic Administration (GHME2015GC01). The authors also acknowledge the support of the UK's Engineering and Physical Sciences Research Council under projects EP/R029423/1 and EP/R007470/1.

Can Zhang is with College of Harbor, Coastal and Offshore Engineering, Hohai University, Nanjing, 210098, China and with Department of Earth Science and Engineering, Imperial College London, London, SW7 2AZ, UK (e-mail: z.can19@imperial.ac.uk).

Stephan C. Kramer is with the Department of Earth Science and Engineering, Imperial College London, London, SW7 2AZ, UK (e-mail: s.kramer@imperial.ac.uk).

Athanasios Angeloudis is with the School of Engineering, Institute for Infrastructure and the Environment, The University of Edinburgh, Edinburgh, EH8 9JU, UK (e-mail: a.angeloudis@ed.ac.uk).

Jisheng Zhang is with College of Harbor, Coastal and Offshore Engineering, Hohai University, Nanjing, 210098, China (e-mail: jszhang@hhu.edu.cn).

Xiangfeng Lin is with College of Harbor, Coastal and Offshore Engineering, Hohai University, Nanjing, 210098, China (e-mail: linxiangfeng@hhu.edu.cn).

Matthew D. Piggott is with Department of Earth Science and Engineering, Imperial College London, London, SW7 2AZ, UK (e-mail: m.d.piggott@imperial.ac.uk).

Digital Object Identifier: <https://doi.org/10.36688/imej.5.273-280>

the tidal turbine array and achieved approximately 6% higher resource from the tidal stream than an empirical based design approach. A gradient-based optimisation method was introduced by Funke et al. [7], in which the micro-siting of individual turbines within an array was optimised in a more flexible way. Only turbine deployment area limits on the location and a minimum distance restriction between turbines were applied. Optimised layouts are unstructured and not simply staggered, which offers greater flexibility [8]–[11]. Notable improvement was achieved when applying this method to the design of the turbine array both in the Inner Sound of the Pentland Firth, UK and around Zhoushan Island, China [7], [12]–[14].

However, among these optimisation studies, it has been assumed that the turbine rotor is always aligned with the upstream velocity direction, which is not the case in practice due to tidal asymmetries and transient changes in the flow direction. Moreover, the yawing mechanism of tidal turbines typically does not allow for a continuous alignment at the same timescales as the tidal flow [15]. The complex interaction between turbines and the influence of yaw angle through wake steering further complicates this picture [16]. Therefore, to obtain the optimal configuration of tidal turbines within an array, one should ideally consider both the locations and yaw angles of individual turbines.

Substantial research into the effects of yaw angles have been conducted in the context of wind turbines. A common finding observed for wind turbines under yaw conditions is that both the generated power and the thrust force decrease with increases in the yaw angle [17], [18]. Through experiments, Adaramola and Krogstad [19] found that when two turbines are operating under optimised yaw conditions over a short distance, the overall efficiency can be improved compared to a larger distance without correcting yaw angles. Dou et al. [20] used a three-dimensional yawed wake model to optimise the power output of a wind turbine farm. They demonstrated that yaw angle optimisation could improve the power yield of an offshore wind farm by up to 7%, with the yaw angle optimisation being more beneficial when streamwise spacing between turbines is small. Along similar lines, Thogersen et al. [21] generalised the Jensen wake model to a statistical meandering wake model. For yaw angle optimisation of the Nysted wind farm, the Jensen wake model yielded a 6.7% improvement in power while the statistical meandering wake model yielded a 7.5% improvement.

There are, however, limited studies on the performance of tidal turbines under yawed conditions. It should be noted that this is often overlooked as most studies often consider idealised studies where flow is imposed in a rectilinear fashion. Baratchi et al. [22] used the actuator line method to simulate a tidal turbine in yawed flow; they demonstrated that values of the turbine power coefficient, C_P , and turbine thrust coefficient, C_t , are lower under yawed compared to non-yawed conditions. Modali et al. [23] studied the performance and wake characteristics of a tidal turbine under yaw using a three-dimensional computational fluid dynamics frame and a k - ω SST turbulence closure

model. They observed that at higher yaw angles, a faster wake recovery is facilitated because of the accelerated interaction between the tip vortices and the skewed wake.

To the best of the authors' knowledge, there has been scarce information about the optimisation of tidal turbines arrays with variable yaw. This paper considers the potential for optimising the turbine array layout, including yaw angles, to increase array power output. Moreover, to overcome the computational load of performing optimisation within a 3D modelling framework, this study introduces yawing effects within a 2D depth-averaged framework. The optimisation includes the influence of alignment on power output of each individual turbine, and a simplified wake steering effect. The optimisation of the turbine layout and its interaction with the hydrodynamics is performed using *Thetis*¹, an open-source coastal ocean modelling framework. *Thetis* has been applied for a number of coastal applications [24], [25]; more details about the *Thetis* model can be found in [26].

II. NUMERICAL MODEL

A. Shallow water equations

In this study, the nonlinear shallow water equations in non-conservative form are used:

$$\begin{aligned} \frac{\partial \eta}{\partial t} + \nabla \cdot (H\mathbf{u}) &= 0, \\ \frac{\partial \mathbf{u}}{\partial t} + \mathbf{u} \cdot \nabla \mathbf{u} - \nu \nabla^2 \mathbf{u} + g \nabla \eta &= -\frac{c_b + c_t}{\rho H} \|\mathbf{u}\| \mathbf{u}, \end{aligned} \quad (1)$$

where η is the free surface displacement, and t is time. H is the total water depth, \mathbf{u} is the depth-averaged velocity vector and ν is the kinematic viscosity of water. The dimensionless coefficient c_b represents bottom friction, which is defined as a constant value in this study. Finally, c_t is an additional parameterisation used to represent turbine thrust and is described in the following section. These equations are solved using the finite element method (FEM) to obtain discrete approximations to the elevation and velocity fields.

B. Turbine model

Linear momentum actuator disc theory (LMADT) is applied in *Thetis* to introduce turbines' thrust and to quantify the energy extraction. A detailed derivation of the approach employed can be found in [27]. The localized thrust force of each turbine is implemented through an enhanced bottom friction coefficient c_t in the form of a Gaussian bump function similar to [7]. There, alongside other optimisation studies following the same technique [8], [9], turbines are assumed to always be optimally aligned with the flow. In this study, however, we seek to incorporate the influence of yaw, where the turbine normal direction is under an angle of θ with respect to the upstream velocity u_0 , as shown in Fig. 1.

¹<https://thetisproject.org/>

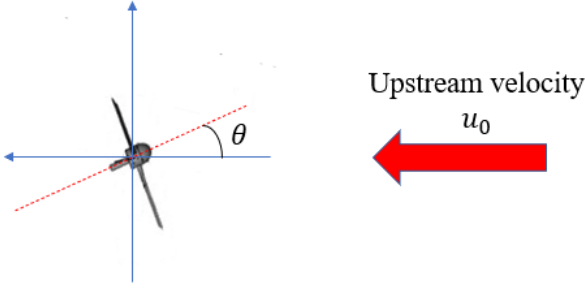


Fig. 1. A diagram displaying the yaw angle of turbine with respect to upstream velocity.

Our implementation is based on a simplified momentum theory which assumes that all forces are applied in the turbine normal direction and any transverse pressure gradients can be neglected. The same LMADT results can then be derived simply considering the turbine-normal component of the upwind velocity: $u_0 \cos(\theta)$.

In particular, we assume a thrust force that takes the following form:

$$F = \frac{1}{2} \rho C_t A_t u_0^2 \cos^2(\theta), \quad (2)$$

where A_t is the turbine cross-sectional area, and C_t a dimensionless thrust coefficient. Under the assumptions above, the following relation between the upwind velocity u_0 and u_1 , the normal component of the ambient velocity through the turbine, can be derived

$$u_1 = \frac{1}{2} \left(1 + \sqrt{1 - C_t} \right) u_0 \cos(\theta), \quad (3)$$

which leads to a predicted power output of

$$P = F u_1 = \frac{1}{4} \left(1 + \sqrt{1 - C_t} \right) C_t A_t \rho (u_0 \cos(\theta))^3. \quad (4)$$

A challenge for the implementation of this turbine model is that for numerical and practical reasons the thrust force needs to be expressed in terms of (the normal component of) the local, numerical flow velocity \hat{u}_1 rather than the upstream velocity u_0 . Further, since this numerical solution \hat{u}_1 is a depth-averaged velocity, it is neither a good approximation of the turbine-normal velocity or of the normal upstream velocity $u_0 \cos(\theta)$. Following [27] however, which uses LMADT to account for the fact that in a depth-averaged model the thrust force is applied over a cross section \hat{A}_t that can be approximated as the product of the turbine diameter and the water depth, an approximate relation between the local depth-averaged numerical solution and the upwind velocity can be derived. Here we follow the same approach in the turbine normal direction which leads to:

$$\hat{u}_1 \approx \frac{1}{2} \left(1 + \sqrt{1 - \hat{C}_t} \right) u_0 \cos(\theta), \quad (5)$$

where \hat{C}_t is a modified thrust coefficient

$$\hat{C}_t = \frac{F}{\frac{1}{2} \rho \hat{A}_t u_0^2 \cos^2(\theta)} = \frac{A_t}{\hat{A}_t} C_t. \quad (6)$$

The enhanced bottom drag term in equation (1) leads to an overall force

$$F = \rho \int c_t \hat{u}_1^2. \quad (7)$$

Substituting equation (5) into equation (7), we obtain F as a function of the upstream velocity u_0 :

$$F = \rho \int c_t \frac{1}{4} \left(1 + \sqrt{1 - \hat{C}_t} \right)^2 (u_0 \cos(\theta))^2. \quad (8)$$

Equating equations (8) and (2), we can solve for the integral $\int c_t$:

$$\int c_t = C_t A_t \frac{4}{\left(1 + \sqrt{1 - \frac{A_t}{\hat{A}_t} C_t} \right)^2}, \quad (9)$$

which determines the overall scaling of the bump function representing each turbine. Substituting equation (5) into equation (4), we derive the expression for power:

$$P = \frac{2 \left(1 + \sqrt{1 - C_t} \right)}{\left(1 + \sqrt{1 - \frac{A_t}{\hat{A}_t} C_t} \right)^3} C_t \rho A_t \hat{u}_1^3. \quad (10)$$

For small angles the thrust force (7) is a reasonable approximation of the force exerted by a yawed turbine [28]. This is however not sufficient for an accurate representation of wake development including wake steering effects behind the turbine. In particular, in under-resolved, depth-integrated/averaged models the deflected wake will almost immediately be redirected in the ambient flow direction due to interaction with the bypass flow. To obtain wake steering effects that take place over larger length scales, such as those observed in higher fidelity, three-dimensional models, we introduce an additional force, similar to that in [29]. This is applied in a direction orthogonal to the flow, so that it does not cause any additional acceleration or deceleration of the flow. Its magnitude is given by

$$F_{\text{extra}} = \frac{1}{2} f^* \rho A_t C_t u_0^2 \sin(\theta) \cos(\theta), \quad (11)$$

where f^* is an overall scaling factor that relates the magnitude to the thrust of the turbine. It should be noted that this factor should be calibrated using data from 3D modelling, lab experiments or field studies in order to simulate turbine wake steering correctly. However, the purpose of this paper is to demonstrate the potential for the optimisation of yaw angle in idealised settings. Therefore here the factor is set somewhat arbitrarily to a value of 30 in order to achieve a reasonable degree of wake steering under yaw conditions.

C. Optimisation method

The shallow water solver in *Thetis* is equipped with a fully automated adjoint that enables the efficient computation of the gradient of a specified outcome of the model, *the functional*, with respect to any input parameters. This gradient information can in-turn be coupled to gradient-based optimisation algorithms and allows us to efficiently solve the problem of improving the layout of tidal turbine formulated as a partial

differential equations (PDEs) constrained optimisation problem [7]:

$$\begin{aligned} & \max_{\mathbf{u}, \eta, d} J(\mathbf{u}, \eta, d), \\ & \text{subject to } \mathcal{F}(\mathbf{u}, \eta, d) = 0, \\ & d_l \leq d \leq d_u, \end{aligned} \quad (12)$$

where $J(\mathbf{u}, \eta, d)$ is the functional of interest; here this corresponds to the combined power output of the turbines. $\mathcal{F}(\mathbf{u}, \eta, d) = 0$ represents the constraint in the form of the non-linear shallow water equations, and \mathbf{u} and η are the numerical velocity and elevation solutions. Finally d is a vector containing the input parameters to optimize for, here a combination of all turbine locations and/or yaw angles. d_l and d_u are lower and upper bounds of the permitted range for turbine locations and/or yaw angles. For any choice of d we can compute the “forward” solution $u(d)$ and $\eta(d)$, and, using the adjoint method, the gradient of $J(\mathbf{u}(d), \eta(d), d)$ with respect to d . The SLSQP algorithm is then applied to perform the optimisation which in addition to the lower and upper bounds is supplied with a minimum distance constraint to avoid turbines being positioned too close to one another. Further details about how this optimisation method works can be found in [7], [13].

D. Study case setup

An idealised rectangular domain is used in this study. As shown in Fig. 2, the considered channel is 2000 m long and 600 m wide. The water depth and viscosity are set as 40 m and $0.001 \text{ m}^2\text{s}^{-1}$ respectively. A 2 m/s constant uniform inflow velocity is set as the boundary condition on the right. At the top and bottom boundaries, the normal velocity component is set to be zero (free slip). A zero elevation condition is applied at the left, outflow boundary. The Turbine Deploying Area (TDA) is located in the centre of the channel, and is 400 m long and 200 m wide. 12 turbines are deployed here in two different initial layouts: an aligned layout and a staggered layout, Fig. 3.

The diameter of each turbine is set to 20 m and the thrust coefficient C_t is assumed to be 0.6. Every turbine has a yaw angle which can vary from -90° to 90° . We assume that 0° means the turbine rotor aligns with the inflow velocity direction (i.e. the x -direction) with the convention that the angle increases as the turbine is rotated counter-clockwise.

First we verify that the numerical thrust of a turbine that is applied in the model corresponds to the analytical LMADT formula (2) on a series of five different meshes. Each of these meshes has a constant mesh resolution inside the TDA which gradually becomes coarser towards the domain boundaries. The details of the five meshes are listed in Table I.

Two different optimisation strategies are considered in this work:

- Fixing the turbine locations and optimising the turbine yaw angles only.
- Optimising the turbine locations as well as the yaw angles simultaneously.

TABLE I
DETAILED INFORMATION ABOUT THE FIVE DIFFERENT MESHES AND THE RMSE BETWEEN THE ANALYTICAL AND NUMERICAL TURBINE THRUST FORCE AMONG THEM AS IN FIG. 4

	Resolution in TDA (m)	Resolution at boundary (m)	RMSE (N)
<i>Mesh 1</i>	2	10	8.21
<i>Mesh 2</i>	5	10	10.94
<i>Mesh 3</i>	5	20	10.90
<i>Mesh 4</i>	5	40	10.90
<i>Mesh 5</i>	10	40	22.70

The initial state of the yaw angles θ for all turbines in both layouts is set to zero, which means the turbine normal is aligned with the velocity direction imposed at the inflow boundary. The minimum distance constraint between turbines is set to be 40 m – twice the turbine diameter.

III. RESULTS AND DISCUSSION

A. Mesh resolution sensitivity analysis

In this study, the numerically predicted turbine thrust against the five different meshes are presented in Fig. 4 and compared with the analytical LMADT formula (2). The root mean squared root errors (RMSE) are summarised in Table I. By comparing the results from Meshes 2–4, we confirm that changing the mesh resolution outside of the TDA region has little effect on numerical turbine thrust values. This can be explained by the fact that outside the TDA region the mesh is required primarily to capture the turbine wake’s recovery, rather than the more intense interactions between flow and turbines. Turbine interactions, which is the focus herein, is restricted within the TDA. Therefore outside the TDA the mesh resolution is expected to have a negligible effect on the value of the numerical turbine thrust. A similar phenomenon was found in [30].

We find that increasing the mesh resolution inside the TDA results in a higher agreement between the turbine thrust and the analytical value. The optimisation procedure requires a number of runs of the “forward” shallow water model and the backward adjoint computation, typically of the order of 70 iterations in the case of combined location and yaw angle optimisation. For this reason, we seek a compromise in terms of accuracy and computational cost, and thus select a mesh resolution of 5 m inside the TDA and 40 m at the boundaries, corresponding to Mesh 4, in all of the following optimisation studies.

B. Optimisation results

The power output before and after the application of different optimisation strategies is summarised in Table II. It can be seen that with the original layouts, the aligned layout yields a power output of 4.17 MW, while the staggered layout yields 6.38 MW. The turbine wakes for these two layouts is displayed in Fig. 5. It can

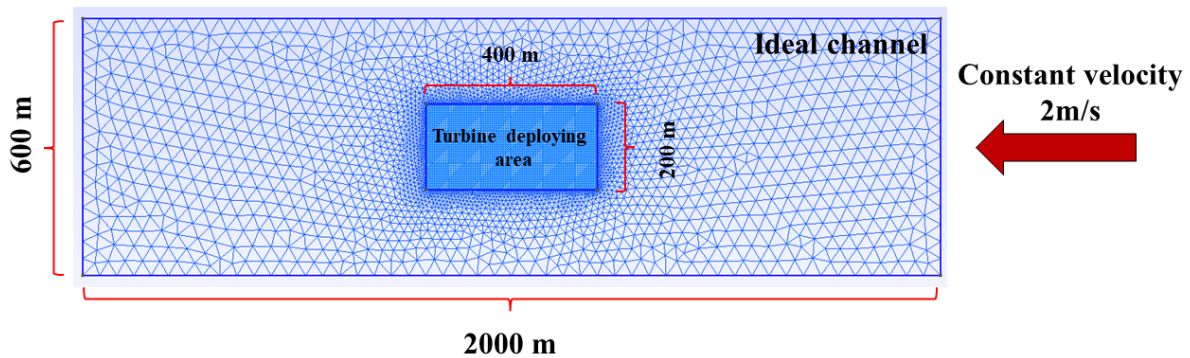


Fig. 2. The mesh of the computational domain with mesh refinement in the Turbine Deploying Area (TDA).

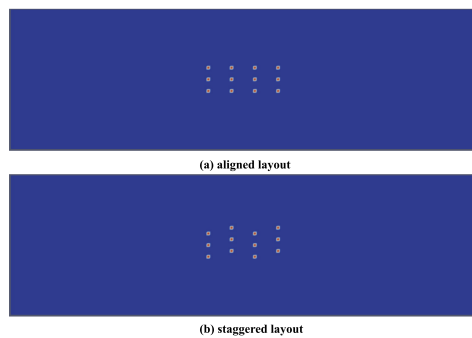


Fig. 3. The aligned and staggered turbine layouts that each contain 12 turbines.

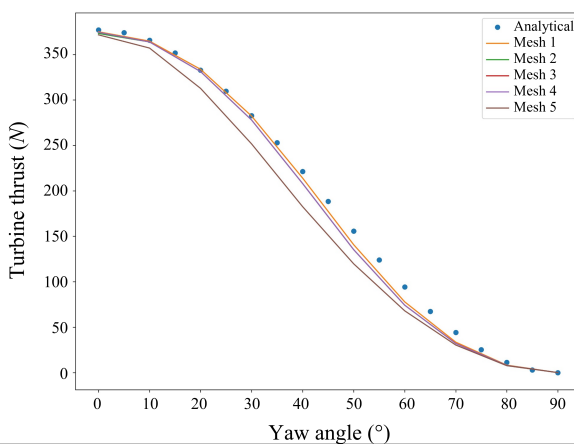


Fig. 4. Numerical turbine thrust for one turbine as a function of yaw angle, comparing five mesh resolutions with the analytical result.

TABLE II
POWER OUTPUTS OF TWO TURBINE ARRAY LAYOUTS BEFORE AND AFTER TWO OPTIMISATION STRATEGIES.

Power outputs (MW)	Aligned layout	Staggered layout
<i>Original layout</i>	4.17	6.38
<i>Optimise angle</i>	7.68	8.27
<i>Optimise layout & angle</i>	12.95	13.47

be clearly seen that the downstream rows making up the turbine array in the aligned layout have low production as the through-turbine velocity is decelerated by the upstream rows. The staggered layout improves this problem significantly by effectively doubling the streamwise distance between interacting turbines, and reducing the cumulative flow deficit effect, so that the wakes are able to better recover before they reach downstream turbines. Thus, the staggered layout is typically a better choice for a turbine array with multiple, fixed rows.

Firstly we consider the optimisation of individual turbine yaw angles while maintaining fixed locations. As shown in Table II, the power output of the aligned layout increases to 7.68 MW, nearly doubled. As for the staggered layout, the power output is improved by about 29.5%. Although the optimised staggered layout still outperforms the optimised aligned layout, the difference has narrowed from 2.21 MW to 0.59 MW. This can be explained by wake steering effects as a consequence of nonzero yaw angles so that turbines in downstream rows of both layouts are able to extract more power from undisturbed or even accelerated (bypass) flow, and that this mitigation is more impactful in the initially aligned case. Although this decreases the output of turbines in the first row, the power generated by the array as a whole is improved. These results

confirm that yawing can be an important factor to consider in turbine array optimisation.

Secondly both turbine locations and yaw angles are optimised simultaneously to improve the whole turbine array power output. Here the aligned and staggered turbine positions are used as a starting point (initial guess) for the optimisation that is allowed to freely move the locations of the turbine within the given constraints of the TDA as well as the minimum distance constraints. Table II shows that the optimised case starting from the aligned layout can generate 12.95 MW of power, which is still slightly smaller than the optimised case which took the staggered layout as the initial condition (13.47 MW) by about 4.0%. Compared with optimising yaw angles only, considering the optimisation of turbine location and yaw angles at the same time achieves a more significant improvement in both cases. It increases the power by more than half – about 68.5% for the aligned layout and 62.9% for the staggered layout.

Although one might expect an identical optimised layout when both turbine locations and yaw angles are considered in the optimisation, this would only be achieved in a truly global optimisation method, which is infeasible given the number of control parameters to optimize for. The SLSQP optimisation method used in this paper obtains significantly improved results in less than a hundred iterations, but its result is a local optimum which means that the original layout may, and here does, affect the optimised result.

Fig. 6 displays the two optimised layouts and their wake distribution. It can be seen that both turbine arrays display a similar funnel-like shape. While the turbines located in the two outer ‘rows’ display significant yaw angles so that the decelerated wake flow is redirected outward so as to not affect the downstream turbines, turbines towards the centre of the array where the flow is accelerated facing the upstream flow more perpendicularly.

IV. CONCLUSION

In this paper, we improve tidal turbine array performance through the optimisation of turbines’ layout and yaw angles. The study is carried out using the *Thetis* model with adjoint based optimisation algorithms. In order to simulate the turbines under yaw conditions, an assumption was made that all forces are applied in the turbine normal direction and any transverse pressure gradients can be neglected. Thus we obtain equations to simulate turbine thrust and calculate power output for different yaw angles.

Two optimisation strategies are considered in this study. We find that when fixing the turbines’ locations and optimising for the turbines’ yaw angles alone, substantial increases in the array’s performance can be obtained. In a highly idealized scenario, if the turbines’ locations as well as yaw angles are optimised at the same time, the power output can be more than doubled compared with their original non-yawed and uniformly aligned performance. This indicates that both turbine location and yaw angle can play an important

role in the ability of a turbine array to generate power, and they should be considered at the same time during the design of the turbine layout.

Although the 2D tidal stream turbine yaw model introduced in this paper shows promising performance, the extra force is an artificial construct that needs further validation. Due to the underlying model assumptions, vertical structure in the turbine wake under yaw condition are unable to be represented due to depth-averaging. Therefore, future work will focus on the development of a 3D yaw turbine model to simulate the turbine and its wake more accurately.

REFERENCES

- [1] D. Coles *et al.*, “A review of the UK and British Channel Islands practical tidal stream energy resource,” *Proceedings of the Royal Society A: Mathematical, Physical and Engineering Sciences*, vol. 477, no. 2255, p. 20210469, 2021. [Online]. Available: <https://royalsocietypublishing.org/doi/abs/10.1098/rspa.2021.0469>
- [2] R. Vennell, S. W. Funke, S. Draper, C. Stevens, and T. Divett, “Designing large arrays of tidal turbines: A synthesis and review,” *Renewable and Sustainable Energy Reviews*, vol. 41, pp. 454–472, 2015.
- [3] Z. Goss, D. Coles, and M. Piggott, “Identifying economically viable tidal sites within the alderney race through optimization of leveled cost of energy,” *Philosophical Transactions of the Royal Society A*, vol. 378, no. 2178, p. 20190500, 2020.
- [4] M. D. Piggott, S. C. Kramer, S. W. Funke, D. M. Culley, and A. Angeloudis, “Optimization of marine renewable energy systems,” in *Comprehensive Renewable Energy, 2nd Edition*. Elsevier, 2021.
- [5] E. González-Gorbeña, A. Pacheco, T. A. Plomaritis, Ó. Ferreira, C. Sequeira, and T. Moura, “Surrogate-based optimization of tidal turbine arrays: A case study for the Faro-Olhão inlet,” in *International Conference on Computational Science*. Springer, 2019, pp. 548–561.
- [6] G. Wu, H. Wu, X. Wang, Q. Zhou, and X. Liu, “Tidal turbine array optimization based on the discrete particle swarm algorithm,” *China Ocean Engineering*, vol. 32, no. 3, pp. 358–364, 2018.
- [7] S. W. Funke, P. E. Farrell, and M. Piggott, “Tidal turbine array optimisation using the adjoint approach,” *Renewable Energy*, vol. 63, pp. 658–673, 2014.
- [8] D. Culley, S. Funke, S. Kramer, and M. Piggott, “Integration of cost modelling within the micro-siting design optimisation of tidal turbine arrays,” *Renewable Energy*, vol. 85, pp. 215–227, 2016.
- [9] R. Du Feu, S. Funke, S. Kramer, D. Culley, J. Hill, B. Halpern, and M. Piggott, “The trade-off between tidal-turbine array yield and impact on flow: A multi-objective optimisation problem,” *Renewable Energy*, vol. 114, pp. 1247–1257, 2017.
- [10] R. Du Feu, S. Funke, S. Kramer, J. Hill, and M. Piggott, “The trade-off between tidal-turbine array yield and environmental impact: A habitat suitability modelling approach,” *Renewable Energy*, vol. 143, pp. 390–403, 2019.
- [11] A. Phoenix and S. Nash, “Optimisation of tidal turbine array layouts whilst limiting their hydro-environmental impact,” *Journal of Ocean Engineering and Marine Energy*, vol. 5, no. 3, pp. 251–266, 2019.
- [12] Y. Wang, Y. Zhai, J. Zhang, L. Tong, S. Song, and T. Zhang, “Numerical study on layout optimization of tidal stream turbines in Zhoushan demonstration project,” in *The 9th International Conference on Asia and Pacific Coasts 2017*, vol. 3. World Scientific, 2017, pp. 278–283.
- [13] C. Zhang, J. Zhang, L. Tong, Y. Guo, and P. Zhang, “Investigation of array layout of tidal stream turbines on energy extraction efficiency,” *Ocean Engineering*, vol. 196, p. 106775, 2020.
- [14] C. Jordan, D. Dundovic, A. Fragkou, G. Deskos, D. Coles, M. D. Piggott, and A. Angeloudis, “Combining shallow-water and analytical wake models for tidal array micro-siting,” 2021.
- [15] M. Piano, S. Neill, M. Lewis, P. Robins, M. Hashemi, A. Davies, S. Ward, and M. Roberts, “Tidal stream resource assessment uncertainty due to flow asymmetry and turbine yaw misalignment,” *Renewable Energy*, vol. 114, pp. 1363–1375, 2017.
- [16] R. Bedard, M. Previsic, O. Siddiqui, G. Hagerman, and M. Robinson, “Survey and characterization tidal in stream energy conversion (tisecc) devices,” *EPRI North American Tidal In Stream Power Feasibility Demonstration Project*, 2005.

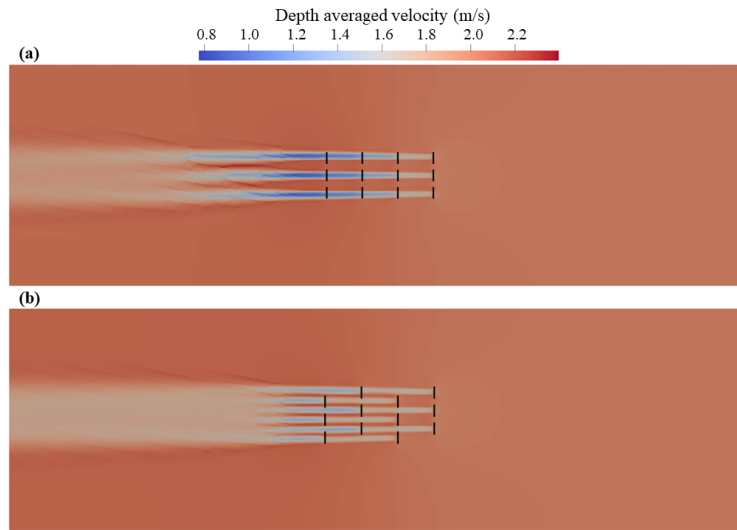


Fig. 5. Velocity distribution of two turbine array layouts in their original states – (a) the aligned layout, (b) the staggered layout.

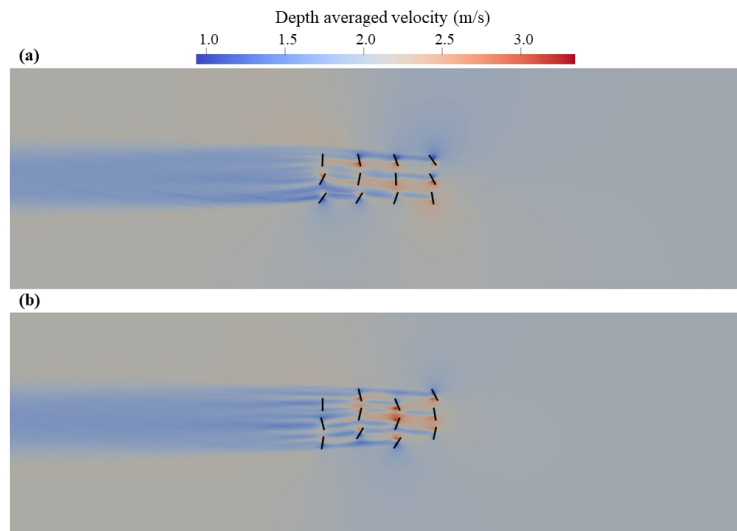


Fig. 6. Velocity distribution of two turbine array layouts after optimising the yaw angle in the case of (a) the aligned layout and (b) the staggered layout.

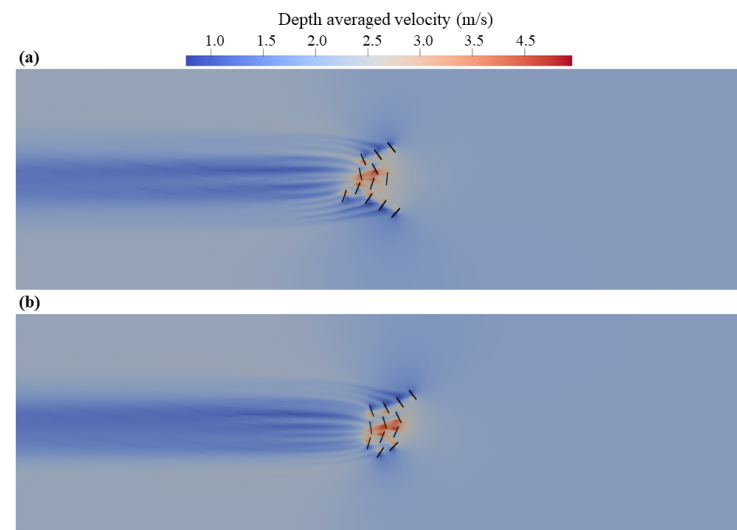


Fig. 7. Velocity distribution of two turbine array layouts after optimising both turbine location and yaw angle, and starting from (a) the aligned layout and (b) the staggered layout.

- [17] M. Bastankhah and F. Porté-Agel, "Experimental and theoretical study of wind turbine wakes in yawed conditions," *Journal of Fluid Mechanics*, vol. 806, p. 506, 2016.
- [18] W. Tian, J. H. VanZwieten, P. Pyakurel, and Y. Li, "Influences of yaw angle and turbulence intensity on the performance of a 20 kw in-stream hydrokinetic turbine," *Energy*, vol. 111, pp. 104–116, 2016.
- [19] M. Adaramola and P.-Å. Krogstad, "Experimental investigation of wake effects on wind turbine performance," *Renewable Energy*, vol. 36, no. 8, pp. 2078–2086, 2011.
- [20] B. Dou, T. Qu, L. Lei, and P. Zeng, "Optimization of wind turbine yaw angles in a wind farm using a three-dimensional yawed wake model," *Energy*, vol. 209, p. 118415, 2020.
- [21] E. Thøgersen, B. Tranberg, J. Herp, and M. Greiner, "Statistical meandering wake model and its application to yaw-angle optimisation of wind farms," in *Journal of Physics: Conference Series*, vol. 854, no. 1. IOP Publishing, 2017, p. 012017.
- [22] F. Baratchi, T. Jeans, and A. Gerber, "Actuator line simulation of a tidal turbine in straight and yawed flows," *International journal of marine energy*, vol. 19, pp. 235–255, 2017.
- [23] P. Modali, N. S. Kolekar, and A. Banerjee, "Performance and wake characteristics of a tidal turbine under yaw," *International Marine Energy Journal*, vol. 1, no. 1 (Aug), pp. 41–50, 2018.
- [24] A. Angeloudis, S. C. Kramer, N. Hawkins, and M. D. Piggott, "On the potential of linked-basin tidal power plants: An operational and coastal modelling assessment," *Renewable Energy*, vol. 155, pp. 876–888, 2020.
- [25] L. Mackie, P. S. Evans, M. J. Harrold, O. Tim, M. D. Piggott, and A. Angeloudis, "Modelling an energetic tidal strait: investigating implications of common numerical configuration choices," *Applied Ocean Research*, vol. 108, p. 102494, 2021.
- [26] T. Kärnä, S. C. Kramer, L. Mitchell, D. A. Ham, M. D. Piggott, and A. M. Baptista, "Thetis coastal ocean model: discontinuous galerkin discretization for the three-dimensional hydrostatic equations," *Geoscientific Model Development*, vol. 11, no. 11, pp. 4359–4382, 2018.
- [27] S. C. Kramer and M. D. Piggott, "A correction to the enhanced bottom drag parameterisation of tidal turbines," *Renewable Energy*, vol. 92, pp. 385–396, 2016.
- [28] T. Burton, D. Sharpe, N. Jenkins, and E. Bossanyi, *Wind energy handbook*. Wiley Online Library, 2001, vol. 2.
- [29] S. Boersma, P. Gebraad, M. Vali, B. Doekemeijer, and J. Van Wingerden, "A control-oriented dynamic wind farm flow model: "wfsim"," in *Journal of Physics: Conference Series*, vol. 753, no. 3. IOP Publishing, 2016, p. 032005.
- [30] C. Zhang, J. Zhang, Y. Wang, T. Zhang *et al.*, "Energy extraction and wake velocity distribution of the turbine array with different layouts," in *The 29th International Ocean and Polar Engineering Conference*. International Society of Offshore and Polar Engineers, 2019.